universität wien

DIPLOMARBEIT / DIPLOMA THESIS

Titel der Diplomarbeit / Title of the Diploma Thesis

„Optical characteristics of the calcifying macroalga *Padina pavonica* along a light gradient“

verfasst von / submitted by

Daniel Lukas Harder

angestrebter akademischer Grad / in partial fulfilment of the requirements for the degree of

Magister der Naturwissenschaften (Mag.rer.nat.)

Wien, 2019/ Vienna, 2019

Studienkennzahl lt. Studienblatt / degree programme code as it appears on the student record sheet:	A 190 445 456
Studienrichtung lt. Studienblatt / degree programme as it appears on the student record sheet:	Lehramtsstudium UF Biologie und Umweltkunde UF Geographie und Wirtschaftskunde
Betreut von / Supervisor:	Ao. Univ.-Prof. Mag. Dr. Michael Schagerl

Abstract

Calcification of water plants is a result of photosynthetic activity. In some groups such as green and red algae, carbonate covers are frequently found, in others such as brown algae, calcification is an exception. We focused on the calcifying phaeophyte *Padina pavonica* and studied optical properties, which are strongly shaped by carbonate cover. It is proposed that the carbonate cover acts as a sun protector with reflecting excess light. Specimens growing at high irradiance should have a thicker calcium carbonate layer due to increased carbonate precipitation than individuals from low light habitats. We moreover expected an increase of thallus absorbance (A) with decreasing reflectance (R) at lower irradiance exposition to optimize light harvesting.

The research was conducted in Rovinj (Croatia) in summer 2018. Specimens were collected from the bay and immediately analyzed in the laboratory of Rudjer Boskovic Institute. We found an absolute increase of thallus area, fresh mass, dry mass and organic mass (OM) with reduced irradiance, but the amount of carbonate per area precipitation did not show the expected reduction at low irradiance. Also, R measurements did not show the expected significant correlation with increasing irradiance exposition. Thallus A stayed constant throughout the light gradient. Transmission (T) however showed an increase with reduced irradiance. This pattern is due to significantly reduced thallus thickness and reduced pigment content and can be explained to minimize the packaging effect. Growing season of the perennial *P. pavonica* thalli is April to September. We were not able to prove light protection via carbonate cover, which might be measurable only later in the year. The larger and heavier specimens in low light habitats suggest higher age of the thalli compared to exposed ones. Low light environments are found in sheltered areas and higher depths. These less disturbed habitats enable survival during storm events.

Keywords: calcification, Padina pavonica, reflectance, photosynthesis, irradiance, environmental conditions

Acknowledgements

Michael Schagerl helped me a lot in both attaining my background research knowledge and in selecting the methodology for my study. He also established the contact with the Institute of Marine Biology, Ruđer Bošković. I thank the employees of the marine biological institute for providing research equipment and for valuable scientific advices. Last but not least, I am very grateful to my colleagues, especially Ana Pfleger, for their support and collaboration.

Table of contents

Introduction

The brown alga species *Padina pavonica* (Linnaeus) Thivy is one of the 75 currently accepted species of this genus (Guiry, 2019). It is placed within the family Dichtyophyceae, and except of *Newhousia imbricata* Kraft, G.W. Saunders, I.A.Abbott & Haroun, the only brown algal taxon which shows calcification (Ni-Ni-Win et al., 2011). *Padina pavonica* is mainly growing in the Mediterranean Sea and in warm regions of the Atlantic Ocean up to southern Britain (Ni-Ni-Win et al., 2011), which implies sensitivity against cold temperature and physical stress (Herbert et al., 2016). *Padina* occurs at rocky shores in the sublittoral characterized by turbulence, high irradiance and tidal currents (Lüning, 1985).

P. pavonica consists of two parts, the annual fronds for photosynthesis and the perennial rhizoid as a holdfast (Pettit et al., 2015). The characteristic fronds up to 15 cm are easily recognized by their fan-shape with alternating brownish and whitish bands (Aisha & Shameel, 2010). On the ventral side of the fronds (oriented to the substrate), the apical tip is enrolled because of the faster growth of the dorsal side. This growth pattern was interpreted to protect young and sensitive cells (Carter, 1927). Fronds start to grow at the marginal meristem (Ni-Ni-Win et al., 2011) and expand sideways (Aisha & Shameel, 2010). The base of *Padina* fronds has up to three layers of cells, while the marginal region has two layers (Bürger et al. 2017).

P. pavonica has concentric arranged hair bands on its surface, with more developed on the dorsal side (Fritsch, 1952). In between these bands, sporangia (sori) covered by a membrane (indusium) are arranged (Garreta & Siguan, 2015). These regions are not calcified and positioned on the ventral surface (Silberfeld et al., 2013). Hairs are assumed to protect the reproductive structures (Fritsch, 1952) and prevent the surface from sand settlement (Carter, 1927) and protect against high irradiance (Thivy, 1959).

Padina has a diplo-haplontic life cycle like most brown algae (Garreta et al., 2007). The morphology of the generations do not differ from each other (isomorph). In order to distinguish between the two generations, gametes or spores have to be present. As a result of this life cycle, two forms of reproduction exist. Haploidic gametes and diploidic spores produced in the fronds, although the fertile sporophyte is much more abundant (Garreta et al., 2007).

Individuals can either be dioecious or monoecious and develop with antheridia and oogonia (Ni-Ni-Win et al., 2011). The mode of preproduction probably depends on temperature. In warm waters, fronds tend to be dioecious, whereas in cold waters, fronds are mostly monoecious (Thivy, 1959). The fronds detach each winter, with the only surviving unit being rhizomes. At suitable conditions in spring, rhizomes sprout and fronds develop again.

P. pavonica is a bioindicator for environmental changes, like pH shifts (Gil-Diaz, 2014) or heavy metal water contents. It is also of interest for industrial purposes, as is has specific properties for biosorption of heavy-metals and therefore may be used in the future to remove or to gain heavy metals (Geraldino et al., 2005). It also has the potential for biodiesel production and as feedstock (Maghraby & Fakhry, 2015). It is already used to monitor trace metals (Campanella et al., 2001), as an anticancer drug (apoptosis of cancer cells can be induced) and other products in the pharmaceutical industry (Bernardini et al., 2018). Moreover, *Padina* has the potential to be used as bioinsecticide (Elbanna & Muhammad, 2011) and shows high antifungal and antioxidant activities caused by its phenolic compounds (Khaled et al., 2012).

Calcareous algae possess a calcifying cover and/or a calcareous skeleton. They show great diversity in aquatic systems and provide information of the history of the earth because they are well suited for fossilization (Wray, 1977). They are used as facies pointers concluding to former water temperature, salinity and water depth. They are petrogenetic and bind sediment to build bioconstructions. Algae can either calcify calcite or aragonite, which is much more soluble. The deposition of calcium salts, generally called calcification is not limited to a specific phylogenetic group. Calcifying representatives are found in green algae, red algae and rarely brown algae, with different mechanisms of calcification being observed. They may occur either extra-, inter- or intracellularly (Martin et al., 2000).

Calcification is not common in Phaeophyceae, which makes *Padina pavonica* interesting to study. *Padina* precipitates $CaCo_3$ in form of extracellular aragonite needles. Macroscopically, these crystals are arranged in concentric stripes mainly on the ventral surface of the thallus (Benita et al., 2018). Although *Padina pavonica* precipitates calcium carbonate, it has no significant contribution to the imposing lime reefs, which developed over millions of years.

The physiological process of calcification is a mechanism to take up and convert bicarbonate (HCO_3^-) into carbon dioxide (CO_2), which is further used in photosynthesis. Due to this process, facilitated by the enzyme carboanhydrase, pH raises. As a side effect, calcium carbonate ($CaCO_3$) is precipitated (Littler & Littler, 1984).

(Photosynthesis: $H^+ + HCO_3^- \rightarrow CO_2 + H_2O \rightarrow CH_2O + O_2$)

(Calcification: $Ca^{2+} + HCO_3^- \rightarrow CaCO_3 + H^+$).

The result out of these two reactions (photosynthesis and calcification) can be summarized with following reaction:

$$Ca^{2+} + 2HCO_3^- \rightarrow CaCO_3 + CH_2O + O_2$$

(McConnaughey & Whelan, 1997)

Thus, the deposition of $CaCO_3$ in aquatic environments highly depends on pH-values, pH-shifts and photosynthetic activity (Littler & Littler, 1984). The optimal pH range for calcification in relation to photosynthesis is between 8,2 and 8,4. In this range, bicarbonate is the dominant inorganic form carbon and the uptake works optimally. If water becomes more alkaline, rates of photosynthesis decrease significantly, due to the more ambient CO_3^{2-} under such conditions and the resulting $CaCO_3$ precipitation. CO_3^{2-} cannot get effectively converted to CO_2. Photosynthetic rates are close to zero at pH 9,5-10,5 (Sand-Jenscn & Gordon, 1984). If seawater is too acidic, carbonate dissolves, which influences calcifying organisms by dissolving carbonate (McConnaughey, 1998).

Different roles of calcification have been augmented. Calcification is suggested to act as mechanical protection against high energy waters. It is also suggested as a protection against grazers or to support photosynthetic carbonate uptake (Benita et al., 2018).

This study focuses on the relationship between optical properties and calcification. Calcification is a result of photosynthetic activity. We therefore expected increased carbonate cover on sun-exposed plants, and a decreasing amount of carbonate content with depth. As carbonate has a whitish appearance, we assumed higher reflectance (R) of high-light exposed thalli compared to low-light plants. We moreover expect a certain pattern between R, transmission (T) and absorbance (A). If more

light is reflected, the less can be transmitted and / or absorbed. We linked calcification and A properties and expected a negative correlation. The more R, the less A. In contrast, increased R could lead to an increased A and reduced T, due to an increased amount of light harvesting pigments as an answer to less available light. Additionally, we expected a negative correlation between T and A. Alternatively, A could increase with increased T due to reduced R and an increased amount of photoactive pigments. T is expected to increase with depth due to lower R and lower amount of carbonate. A is expected to increase with depth, which we divided into light classes, compared to R but not as much as T.
Furthermore, this study focuses on the correlation between the amount of carbonate per area and size and age of the plant, respectively. The assumption is that deeper plants have larger surface areas because these plants have more time to grow under undisturbed environmental factors, although less light is available. So, a positive correlation between calcification and age is expected. The specific carbonate content (carbonate based on unit area) should not change with depths.

Material and methods

Study site

The study was performed in the bays around Rovinj located in the Adriatic Sea (Croatia - 45°04'58.4"N 13°38'12.1"E) in June 2018. The coastline of this region is represented by the Adriatic Carbonate Platform forming impressive karst formations in Istrian and the Croatian Karst Dinarides. We took fronds from depths between 0.1 to 11.3 m by snorkeling, scuba and apnea diving. Depths were measured by a diving computer (*SUUNTO FAVOR).* Irradiance was measured by HOBO Pendant Temperature/Light 64K Data Loggers attached to diving weights at each sampling site. For surface irradiance, a reference HOBO was positioned above the water surface at a sun light exposed spot. We then calculated light classes (LC) based on the percentage of surface light (relation between underwater *HOBO* and surface *HOBO)*: LC1 > 25%, LC2 ≤ 25% to >10%, LC3 ≤ 10% to >5 %, LC4 ≤ 5%.

After collecting material, specimens were immediately transferred to the marine biological institute of Rovinj, the “Ruđer Bošković laboratory”, were measurements were conducted. Each *Padina* frond was divided into two parts, and then

photographed with digital imaging for surface area measurements. Calculation of frond areas were conducted by the *ImageJ-Software.* Afterwards, both parts of each frond were blotted off to remove surface water and then weighed with scale Mettler MT5 for fresh mass (FM). One part of the respective frond was further used for pigment analysis (Pfleger, 2019), while the other one was used for measurements of optical properties, carbonate content and dry mass (DM). Mean R values were measured over the spectrum from 400nm to 700nm. For these measurements, via spectroradiometer (Ocean Optics: USB4000 Miniature Fiber Optic Spectrometer), a tripod was used to standardize the distance between the R probe and the frond surface. To avoid artefacts due to water R, measurements were taken in sea water. Reference measurements were conducted by using a white standard (Ocean optics: WS-1-SL Reflectance Standards). R (%) was calculated in relation to reference measurement (R = frond measurement / reference measurement * 100). T was measured with natural light (blue sky, no direct sunlight) to avoid scattering artefacts. First, irradiance without the frond was measured and taken as 100% incoming light. Then T was measured by placing fronds in front of the fibre optics (Ocean Optic: USB4000 Miniature Fiber Optic Spectrometer; T = frond measurement/reference measurement * 100). A was calculated as follows: A = 100 – R – T. Afterwards, fronds were put into a dry locker overnight (95°C) and DM measured. Water content (WC) was calculated (FW – DW).

For the carbonate layer, we first removed the carbonate from dried material by using 20% (v/v) -acetic acid (CH_3COOH) followed by rinsing with tap water. Fronds were then put into the dry locker again. Weight of the remaining parts was then measured and carbonate content (in %) was calculated as follows: CC = (DM – DM decalcified) / DM * 100). Organic mass OM was calculated (DM – CC).

Statistics

Statistics were conducted with the software package SigmaPlot 12.5 (Systat Software, San Jose, CA, USA) and Microsoft Excel (Office 365 ProPlus).

Normal distribiution was tested by using Kolmogorov-Smirnov test.

For correlations between two parameters, linear regression analyses was conducted.

The correlation of more than two parameters, which were normally distributed (Kolmogorov-Smirnov test), and which had variance homogeneity (Levene's test), one-way ANOVA was conducted. If there was no normal distribution or no variance homogeneity, Kruskal-Wallis test non-parametric) were conducted, with post-hoc-, Dunn's-, and Tukey-Kramer- tests, respectively.

Results

Light and depth correlate significantly with each other (Fig. 1), which justifies to interpret LC also as depth gradient.

FM and DM are significantly increasing from LC1 until LC3, but they decrease from LC3 to LC4 (Tab. 1). Also frond area increases significantly from LC1 to LC3 and then decreases in LC4. WC increases from LC1 until LC3 but less than FM and DM Tab. 2). Frond carbonate cover increases significantly with LC (Tab. 2; Fig. 2), with area (Fig. 3) and with DM (Fig. 4), but no significant changes of $CaCO_3$ content per thallus area with LC were calculated (Fig. 5). $CaCO_3$ content per DM increases significantly with LC (Fig. 6). That means, that algae have higher area values and are heavier along LC1 to LC3. At LC4, *Padina* fronds become smaller and the mass (FM, DM, WC, OM) decreases. According to this, absolute carbonate content per frond increases until LC3 and drops down at LC4, whereas the relative amounts of carbonate based on frond area, and fronds mass, respectively, keep stable

When looking at the overall R spectra, the maximum was measured at 400nm. R first decreased from 400nm until a minimum at 680nm. Than R increases slightly until 700nm. Between 400nm and 700nm, mean R (%) of specimens from LC1 was the highest, whereas algae of LC4 showed the lowest R (Fig. 7). A significant negative correlation was measured between LCs and R (Figs. 7, 8), and carbonate cover and R We however found no significant changes between R and carbonate cover per unit area (Figs. 9, 10).

T increases significantly with increasing LC (Figs. 11, 12). T spectra mirror the A spectra (Figs 12, 14). T decreases between 400nm and 500nm, followed by an increase until 600nm. It decreases with a minimum at 630nm and then raises again 680nm and raises until 700nm (Figs. 12,). A show a decreasing trend with increasing LC, although these changes are not significant (Tab. 3). A significant negative correlation with T is however evident (Fig. 13). A decreases slightly and less than R with LC (Tab 3). A and R have a significant negative correlation to each other (Fig. 15). A decreases significantly with increasing R.

While R does not change significantly in relation to LC and carbonate per area, T increases with LC and carbonate per area. A shows opposite results by decreasing slightly (not significantly) with LC and carbonate per area.

Disscussion

Algae growing in rocky, sublittoral areas face various challenges such as, low amount of nutrients, high irradiance, strong current forces, high pressure of grazers and space competition. To cope with these adverse conditions, several morphological and physiological adaptations are necessary.

Algae in near-surface environments are exposed to high irradiance. They developed protection measures against photooxidation, like photoprotective pigments (Havaux & Niyogi, 1999). and mechanism to facilitate nutrition uptake (McConnaughey & Whelan, 1997). Against grazers, algae need structural, morphological and/or chemical defense mechanisms (Padilla, 1989). Different studies assume for *Padina pavonica* that the overall response of all these stress factors is calcification (Padilla, 1989; McConnaughey & Whelan, 1997; Kingsley, 1989). The carbonate layer is highly affecting optical properties of the thallus.

Light and depth correlate significantly with each other (Fig. 1), which justifies interpreting LC also as depth gradient. To increase R, the carbonate layer serving as a protection against photooxidation and high irradiance stress should be thicker in sun-exposed algae than in shaded algae. At low intensity of irradiance (in deeper regions) carbonate may dissolve easier, due to reduced photosynthetic activities and reduced respiration (Beer & Larkum, 2001). We however were not able to detect significant changes of R along the LCs in terms of carbonate cover per unit area (Fig. 10). Furthermore, there were no significant changes of calcium carbonate content per area in all LCs, which explains the results of R (Fig.5). These results, together with an absent correlation between R and carbonate per area, lead to the assumption, that not only the amount of carbonate is relevant for R, but also, structural characteristics of the aragonite crystals seem to be essential. Needle-shaped crystals cover younger parts of the thallus, while older parts are covered by crystals, which have lost their needle-shape. The aragonite crystals are small and randomly oriented (M. A. Borowitzka et al., 1974). The main growing season of *Padina pavonica* in the Mediterranean Sea is from June to September (Ali et al., 2010), which implies that the calcium carbonate layer was just at the beginning of its development. According to Bürger & Schagerl (2010), the amount of calcium carbonate is significantly higher in autumn than at the beginning of the growing season, same for R (Bürger et al.,

2017). Young specimens were just starting to precipitate carbonate. Moreover, carbonate dissolution is enhanced by lower temperature (Bürger, 2010).

For green algae, such as *Halimeda*, calcification is only initiated if chloroplasts reach a specific, functional maturity (Borowitzka & Larkum, 1977), which implies a link between carbonate precipitation and photosynthesis. In *Halimeda,* rates of calcification are higher in younger thalli lower amounts of carbonate were observed in older, basal regions of the thallus. In older parts, photosynthetic rates were lower and respiration was higher (Borowitzka & Larkum, 1977).

Calcification might act as a sun protector because of the lack of absorbing components like MAAs (mycrosporine-like amino acids). MAAs belong to the most common compounds, which act as sunscreen in various terrestrial and marine organism (Karsten et al., 1998). The MAA-content correlates positively with the doses of UV (Shick et al., 1995). In contrast, deep water algae like Phaeophyceae, do not contain MAAs or just traces of it (Karsten et al., 1998).

A result of marine acidification due to CO_2 enrichment is that carbonate is dissolved. This reaction also affects calcifying organisms like *Padina*. *Padina* however seems not to suffer in such areas (Gil-Diaz et al., 2014). Under conditions of decreasing pH due to ocean acidification measured in the last three decades, *Padina* strongly reduced its $CaCO_3$ coverage(Gil-Diaz et al., 2014). *Padina* adapted its physiology, acting like a sun-adapted plant and not like a shade-adapted species, which could explain its thriving success under low pH conditions (Betancor et al., 2014). On the other hand, the previously mentioned conditions lead to reduced synthesis of phenolic compounds, which make fronds more palatable for herbivores (Alstyne & Paul, 1990). Moreover, loss of carbonate could also reduce mechanical resistance against grazers. The abundance of *Padina* also depends on the coexistence with organisms influenced by ocean acidification (LITTLER, 1976). Sea urchins, which are major grazers of *Padina,* are highly affected by ocean acidification. The increased mortality of sea urchins and its significantly reduced abundance in regions with low pH, can explain the benefit and the success of *Padina* in those regions. There is also a positive effect on photosynthesis and productivity due to lower pH, higher CO_2 content respectively. Higher contents of chlorophylls a and c had been found in fronds of CO_2 enriched waters, effecting photosynthetic response on ocean acidification. At CO_2 supersaturation, rETR-max and mean rETR-max were increased

(Johnson et al., 2012). This positive effect on photosynthesis due to the enhanced carbonate fixation however stimulates calcification (Johnson et al., 2012; Borowitzka, 1982).

Betancor et al. (2014) compared *Padina* and *Lobophora variegate* (an non calcifying alga) and were able to show that both taxa suffer from a decrease of photoprotective compounds and from a reduction of antioxidant activities. While *Padina* additionally showed decalcification, its optimum quantum yield remained unaffected. *Padina* acclimates to lowered pH through an increased onset of light saturation (Betancor et al., 2014).

In summary *Padina* is very sensitive to chronic ocean acidification, acting like a sun adapted plant and not like a shade adapted alga. This could be a response to a more sun exposed thallus due to a reduce carbonate coverage. This argues for calcification as irradiance adaptation, even though the thriving of *Padina* seems to be supported at conditions of lower pH values and higher carbonate dissolubility respectively (Gil-Diaz, 2014)

Beside chlorophylls a and c, *Padina pavonica* contains various carotenoids, like fucoxanthin as major accessory pigment. This latter pigment is responsible for the brownish color. Around 665 nm and 430 nm chlorophyll a shows A maxima, while chlorophyll c has its maxima at 630, 585 and 450 nm. Fucoxanthin also preferable absorbs around 450 nm. (Wright et al. 1991; Wang et al., 2018) The measured A spectra clearly fit together with these maxima and with the R minima (Figs. 7, 14). We conclude that R is also influenced by inner structures of the thallus, not only from the surface. R of algae surface is comparable with coral surfaces (Enríquez et al., 1994). Also, Bürger (2010) has shown a rise in the R-spectra of *Padina*, between 560 and 600 nm and a drop at 670 nm. Our results showed a slight rise 500 and 600 nm and drop at around 650 nm, which is similar. The 650 nm drop is caused by A of chlorophyll a (Gitelson, 1993). Fucoxanthin and chlorophyll c are responsible for the drop of the R between 400 and 500 nm (Bürger et al., 2017). Also, the increasing amounts of carbonate per DW with LC, together with a decreasing R with LC, argues against carbonate as only important factor for R.

Reasons for the results of non-existing calcification and R correlation could be, that calcification is just product of metabolism, which has no specific function or could be that calcification has other benefits. One assumption is that calcification acts as a

mechanical support (Stenek, 1982). Other studies found out, that the role of calcification against animal feeding is low, because calcification makes the plant more fragile (Padilla, 1989) . However, chemical defense mechanisms in *Padina* are probably connected to calcification (Hay, 1994). Another study showed a negative correlation between size of *Padina* and the number of herbivores fish and sea urchins around the plants (Hereu, 2006). Although we did not focus on animal feeding, but more on optical properties in relation with calcification.

The absolute amount of calcium carbonate clearly correlates with FM, DM, OM, WC, and frond size (Figs. 3, 4, Tab.1, Tab. 2). All these parameters increase significantly between LC1 and LC3 and then decrease at LC4. Algae growth is influenced by irradiance and by nutrition supply, temperature and biotic interactions. In areas characterized by high temperature and high irradiance, the density of *Padina* is high, constraining large thallus growth. According to this, in deeper areas with less irradiance and lower temperatures specimen have more space to grow and develop larger thalli (Creed et al., 1997). Also, wave action might result in smaller thallus size. We therefore assume that large specimens from deeper areas are older due to slow, undisturbed growth conditions.

After start of the growing in spring, biomass and carbonate coverage increases during summer and autumn with higher temperature (Einav et al., 1995). Aragonite starts to develop in the intracellular space, in regions where also chloroplasts occur (Okazaki et al., 1986). This argues for the initiation of calcification due to photosynthesis (Johnson et al., 2012) and for the increase of carbonate per DW in undisturbed low light areas (Fig 6). Due to this link, strong decalcification, even in very low pH regions, gets offset by elevated photosynthesis and it's calcification inducing function under high CO_2-conditions (Hofmann et al., 2011).
The decrease of A with LC can be explained by thallus thickness, which, according to Bürger (2010), is higher in areas with high irradiance. Thinner thalli are located in deeper waters (Bürger, 2010). According to this, our samples form low light regions, contain more carbonate compared to organic mass (OM) and WC (Fig. 16). Thicker thalli might be an adaptation to wave action and desiccation near the water surface, making the plants more robust (Littler & Littler, 1980). Beside this, thallus thickness might also act as a sun protector. A increases mainly due to thallus thickness, and the amount of chlorophyll a, but thallus thickness increases A much more effective than the amount of chlorophyll a. The amount chlorophyll a increases with thallus

thickness but not linearly (Enríquez et al., 1994). Thicker thalli show increased total A. But thinner thalli, with similar chlorophyll a content, capture more irradiance per unit biomass. A per unit biomass reflects the efficiency of carbon turnover and photosynthesis. Thick thalli absorb less light per unit biomass than thin thalli with similar chlorophyll a content. Therefore thin thalli develop larger photosynthetic surfaces per unit fixed carbon and grow more due to a lower minimum light requirement than thick thalli (Ramus, 1990). Therefore thin thalli have advantages in photosynthesis, reproduction and growth (King & Schramm, 1976). An explanation for this could be the reduced package effect. Thin thalli have less photoactive pigments, which work more effectively, due reduced pigment self-shading (Raven, 1984). This fits together with the observations of Pfleger (2019), who measured reduced pigment content in *P. pavonica* thalli in higher depths.

Although pigment content is less responsible for A than thallus thickness, it still plays a role and can explain the comparable amounts of carbonate ($CaCO_3$/area) in each LC. According to Pfleger (2019), the amount of photoactive pigments (chlorophyll a, c and fucoxanthin) and light protective pigments (β-carotenoids) of *P. pavonica* decrease with increasing LC. According to this finding, ETRmax (maximum electron transport rate) also decreases with increasing LC (Pfleger, 2019). The higher amount of photosynthetic pigments and the higher ETRmax values at the water surface leads to the assumption, that these plants are adapted to more irradiance, compared to deeper growing algae or that thalli could be larger at the water surface as response to more photosynthetic activity. In contrast, our measurements show larger and heavier thalli with LC increasing from LC1 to LC3. This pattern can be explained by high wave action near the water surface and the high density of *Padina* in areas with high irradiance, encumbering thallus growth. *Padina* thalli were larger and heavier but, according to Bürger, thinner with increasing LC, which explains the increased T values with LC (Tab. 3).

Conclusion

We expected that calcification acts as a protector against excess irradiance. Therefore, the amount of calcium carbonate and R respectively, should be higher in sun exposed areas. Moreover, T should be higher in regions with low R and A should stay at a constant level (but increased in relation to R), due to an expected negative correlation to both, R and T.

In conclusion, T and A show the expected results. T increases with less irradiance supply, whereas A remains at a constant level. R however is not responsible for this pattern, but rather thallus thickness and pigment content, which both decrease with depth. R decreases slightly, but still significantly with depth. Carbonate cover per unit area increases only slightly, whereas carbonate per DM increases more clearly with increasing LC. Changing composition of thalli, with increasing LC, with higher amounts of carbonate per DM and relatively decreased amount of WC and OM, could be the reason for thinner thalli, for an increased T and for the slightly decreased R. Our hypothesis of calcification as a sun protector could not be confirmed. The results of Bürger (2010), who described decreasing carbonate cover in autumn and appropriate (lower) R values in low irradiance areas, argue for calcification as an irradiance protector. In contrast, the fact that calcification takes place during the night, at almost the same level argues against this, calcification acts as a sun protector, hypothesis. Also, the thriving success of *P. pavonica* in acidified region of the ocean, with reduced carbonate layer and the fact that the deepest growing algae in the world are calcifying are arguments against the sunscreen hypothesis. Calcification might be an adaptation that optimizes photosynthesis in intermediate alkaline waters at an optimal pH range for calcification between 8,2 and 8,4, especially in autumn when the days are getting shorter. Due to the increase of carbonate during the growing season, calcification may act as a mechanism to finish the annual life cycle of *Padina*, which would also be a kind of a sun protection, comparable to the terrestrial leaf color changes. Further studies, which should take place in the laboratory, are necessary, especially about R influencing characteristics of *P. pavonica,* to find out how calcification is influenced by irradiance.

References

Aisha, K., & Shameel, M. (2010). OCCURRENCE OF THE GENUS PADINA (DICTYOPHYCEAE , PHAEOPHYCOTA) IN THE COASTAL WATERS OF KARACHI. *Department of Botany, University of Karachi*, *42*, 319–340.

Ali, A. I., Ktari, L., Boudabbous, A., & Bour, M. E. L. (2010). SEASONAL VARIATION OF ANTIBACTERIAL ACTIVITY OF THE BROWN ALGA PADINA PAVONICA (L) THIVY COLLECTED FROM NORTHERN COAST OF TUNISIA. Bull. Inst. Natn. Scien. Tech. Mer de Salammbô. 37. 111–116.

Alstyne, K. L. Van, & Paul, V. J. (1990). Polyphenolic Compounds in Marine Macroalgae : Temperate Brown Algal Defenses Deter Feeding by Tropical Herbivorous Fishes Oecologia The biogeography of poly phenolic compounds in marine macroalgae, *84*(2), 158–163.

Amelia Gómez Garreta, Jordi Rull Lluch, M. C. B. M. & M. A. R. S. (2007). On the presence of fertile gametophytes of Padina pavonica (Dictyotales , Phaeophyceae) from the Iberian coasts by, *64*(1), 27–33.

Beer, D. De, & Larkum, A. W. (2001). microsensors Photosynthesis and calcification in the calcifying algae Halimeda discoidea studied with microsensors, (October 2018). https://doi.org/10.1046/j.1365-3040.2001.00772.x

Benita, M., Dubinsky, Z., & Iluz, D. (2018). Padina pavonica: Morphology and Calcification Functions and Mechanism. *American Journal of Plant Sciences*, *09*(06), 1156–1168. https://doi.org/10.4236/ajps.2018.96087

Bernardini, G., Minetti, M., Polizzotto, G., Biazzo, M., & Santucci, and A. (2018). Pro-Apoptotic Activity of French Polynesian Padina pavonica Extract on Human Osteosarcoma Cells. *Marine Drugs*, *16*(12). https://doi.org/10.3390/md16120504

Betancor, S., Tuya, F., Gil-Díaz, T., Figueroa, F. L., & Haroun, R. (2014). Effects of a submarine eruption on the performance of two brown seaweeds. *Journal of Sea Research*, *87*, 68–78. https://doi.org/10.1016/j.seares.2013.09.008

Borowitzka, M. A., Larkum, A. W. D., & Nockolds, C. E. (1974). A scanning electron microscope study of the structure and organization of the calcium carbonate deposits of algae. *Phycologia*, *13*(3), 195–203. https://doi.org/10.2216/i0031-8884-13-3-195.1

Borowitzka, Michael A. (1982). Morphological and Cytological Aspects of Algal Calcification. *International Review of Cytology*, *74*(C), 127–162. https://doi.org/10.1016/S0074-7696(08)61171-7

Borowitzka, Michael A., & Larkum, A. W. D. (1977). CALCIFICATION IN THE GREEN ALGA HALIMEDA. I. AN ULTRASTRUCTURE STUDY OF THALLUS DEVELOPMENT. *Journal of Phycology*, *13*(1), 6–16. https://doi.org/10.1111/j.1529-8817.1977.tb02879.x

Bürger, K. (2010). Optical properties in relation to the carbonate layer and morphological studies of the brown alga Padina pavonica (L.) Thivy.

Bürger, K., Clifford, E. L., & Schagerl, M. (2017). Morphological changes with depth in the calcareous brown alga Padina pavonica. *Botanica Marina*, *60*(2), 171–180. https://doi.org/10.1515/bot-2016-0069

Campanella, L., Conti, M. E., Cubadda, F., & Sucapane, C. (2001). Trace metals in seagrass , algae and molluscs from an uncontaminated area in the Mediterranean. *Environmental Pollution*, *111*, 117–126.

Carter, P. W. (1927). The life-history of padina pavonia. *Annals of Botany*, *os-41*(1), 139–160. https://doi.org/10.1093/oxfordjournals.aob.a090060

Creed, J. C., Norton, T. A., Jones, J. M. K., Erin, P., Erin, P., Man, I., & Ja, I. M. (1997). Intraspecific competition in Fucus serratus germlings: The interaction of light, nutrients and density 1 ,. *Journal of Experimental Marine Biology and Ecology*, *212*, 211–223.

Einav, R., Breckle, S., & Beer, S. (1995). Ecophysiological adaptation strategies of some intertidal marine macroalgae of the Israeli Mediterranean coast. *MARINE ECOLOGY PROGRESS SERIES*, *125*, 219–228.

Elbanna, S. M., & Muhammad, M. H. (2011). Screening of some seaweeds species from South Sinai, Red Sea as potential bioinsecticides against mosquito larvae; Culex pipiens. *EAJBS*, *4*(2), 21–30.

Enríquez, S., Agustí, S., & Duarte, C. M. (1994). International Association for Ecology Light Absorption by Marine Macrophytes Published by : Springer in cooperation with International Association for Ecology Stable URL : http://www.jstor.org/stable/4220676. *Ecology*, *98*(2), 121–129.

Fritsch, F. E. (1952). *No TitleThe structure and reproduction of the algae : 2 : Foreword, Phaeophyceae, Rhodophyceae, Myxophyceae*. *Cambridge : Univ. Press*.

Garreta, A. G., & Siguan, M. A. R. (2015). Padina ditristromatica and Padina pavonicoides (Dictyotales , Phaeophyceae): two new records for the marine benthic flora, *36*(1), 55–63. https://doi.org/10.7872/crya.v36.iss1.2015.55

Geraldino, P. J. L., Liao, L. M., & Boo, S. M. (2005). Morphological Study of the Marine Algal Genus Padina (Dictyotales , Phaeophyceae) from Southern Philippines : 3 Species New to Philippines. *Algae*, *20*(2), 99–112.

Gitelson, A. (1993). Algorithms for remote sensing of phytoplankton pigments in inland waters. *Advances in Space Research*, *13*(5), 197–201. https://doi.org/10.1016/0273-1177(93)90545-M

Havaux Michael and Niyogi, K. K. (1999). The violaxanthin cycle protects plants from photooxidative damage by more than one mechanism, *96*(July), 8762–8767.

Herbert, R. J. H., Ma, L., Marston, A., Farnham, W. F., Tittley, I., & Cornes, R. C. (2016). The calcareous brown alga Padina pavonica in southern Britain: population change and tenacity over 300 years. *Marine Biology*, *163*(3), 1–15. https://doi.org/10.1007/s00227-015-2805-7

Hereu, B. (2006). Depletion of palatable algae by sea urchins and fishes in a Mediterranean subtidal community. *Marine Ecology Progress Series*, *313*, 95–103. https://doi.org/10.3354/meps313095

Hofmann, G. E., Smith, J. E., Johnson, K. S., Send, U., Levin, L. A., Paytan, A., … Martz, T. R. (2011). High-Frequency Dynamics of Ocean pH : A Multi-Ecosystem Comparison. *PLoS ONE*, *6*(12). https://doi.org/10.1371/journal.pone.0028983

Johnson, V. R., Russell, B. D., & Fabricius, K. E. (2012). Temperate and tropical brown macroalgae thrive , despite decalcification , along natural CO 2 gradients. *Global Change Biology*, *18*, 2792–2803. https://doi.org/10.1111/j.1365-2486.2012.02716.x

Karsten, U., Sawall, T., Hanelt, D., Bischof, K., Figueroa, F. L., Flores-moya, A., & Wiencke, C. (1998). An Inventory of UV-Absorbing Mycosporine-Like Amino Acids in Macroalgae from Polar to Warm-Temperate Regions, *41*, 443–453.

Khaled, N., Hiba, M., & Chbani, A. (2012). Antioxidant and Antifungal activities of Padina Pavonica and Sargassum Vulgare from the Lebanese Mediterranean Coast Naja Khaled , Mawlawi Hiba , Chbani. *Environmental Biology*, *6*(1), 42–48.

King, R. J., & Schramm, W. (1976). Photosynthetic Rates of Benthic Marine Algae in Relation to Light Intensity and Seasonal Variations *, *222*(37), 215–222.

Littler, M. M. (1976). Calcification and its Role among the Macroalgae 1, *12*(1), 27–41.

Littler, M. M., & Littler, D. S. (1984). Models of Tropical Reef Biogenesisz The Contribution of Algae. *Phycoiogica! Research*, *3*.

Lüning, K. (1985). *Meeresbotanik*. Stuttgart: Georg Thieme Verlag.

Maghraby, D. M. El, & Fakhry, E. M. (2015). ScienceDirect Lipid content and fatty acid composition of Mediterranean macro-algae as dynamic factors for biodiesel production §. *Oceanologia*, *57*(1), 86–92. https://doi.org/10.1016/j.oceano.2014.08.001

Mark E . Hay, Q. E. . K. and W. F. (1994). Synergisms in Plant Defenses against Herbivores : Interactions of Chemistry , Calcification , and Plant Quality. *Ecology*, *75*(6), 1714–1726.

Mark M . Littler and Diane S . Littler. (1980). The Evolution of Thallus Form and Survival Strategies in Benthic Marine Macroalgae : Field and Laboratory Tests of a Functional Form Model. *The Universtity of Chicago Press Jornals*, *116*(1), 25–44.

Martin, C., Bischof, N., & Eiblmaier, M. (2000). Kalkalgen. *Spektrum Akademischer Verlag, Heidelberg,* https://www.spektrum.de/lexikon/geowissenschaften/kalkalgen/7948. Zugriff: 08.10.2018

McConnaughey, T. (1998). Acid secretion, calcification, and photosynthetic carbon concentrating mechanisms. *Canadian Journal of Botany*, *76*(6), 1119–1126. https://doi.org/10.1139/b98-066

McConnaughey, T. A., & Whelan, J. F. (1997). Calcification generates protons for nutrient and bicarbonate uptake. *Earth-Science Reviews*, *42*(1–2), 95–117. https://doi.org/10.1016/S0012-8252(96)00036-0

Ni-Ni-Win, Hanyuda, T., Arai, S., Uchimura, M., Prathep, A., Draisma, S. G. A., … Kawai, H. (2011). A taxonomic study of the genus padina (dictyotales, phaeophyceae) including the descriptions of four new species from japan, hawaii, and the andaman sea. *Journal of Phycology*, *47*(5), 1193–1209. https://doi.org/10.1111/j.1529-8817.2011.01054.x

Okazaki, M., Pentecost, A., Tanaka, Y., & Miyata, M. (1986). A study of calcium carbonate deposition in the genus padina (Phaeophyceae, dictyotales). *British Phycological Journal*, *21*(2), 217–224. https://doi.org/10.1080/00071618600650251

Padilla, D. K. (1989). ALGAL STRUCTURAL DEFENSES: FORM AND CALCIFICATION IN RESISTANCE TO TROPICAL LIMPETS‘. *Ecology*, *70*(4), 835–842.

Pettit, L. R., Smart, C. W., Hart, M. B., Milazzo, M., & Hall-spencer, J. M. (2015). Seaweed fails to prevent ocean acidification impact on foraminifera along a shallow-water CO 2 gradient. *Ecology and Evolution*, *5*(9), 1784–1793. https://doi.org/10.1002/ece3.1475

Ramus, J. (1990). A form-function analysis of photon capture for seaweeds. *Hydrobiologia*, *204*(205), 65–71.

Raven, B. J. A. (1984). A Cost-Benefit Analysis of Photon Absorption by Photosynthetic Unicells. *Wiley on Behalf of the New Phytologist Trust*, *98*(4), 593–625.

Rowan Kingsley S. (1989). *Photosynthetic Pigments of Alga*. Cambridge: Cambridge University Press.

Sand-Jenscn, K., & Gordon, D. M. (1984). Differential ability of marine and freshwater macrophytes to utilize HCO and COs. *Marine Biology*, *80*, 247–248.

Shick, J. M., Lesser, M. P., Dunlap, W. C., Stochaj, W. R., Chalker, B. E., & Wu Won, J. (1995). Depth . dependent responses to solar ultraviolet radiation and oxidative stress in the zooxanthellate coral Acropora microphthalma. *Marine Biology*, *122*, 41–51.

Silberfeld, T., Bittner, L., Fernández-García, C., Cruaud, C., Rousseau, F., de Reviers, B., … De Clerck, O. (2013). Species Diversity, Phylogeny and Large Scale Biogeographic Patterns of the Genus Padina (Phaeophyceae, Dictyotales). *Journal of Phycology*, *49*(1), 130–142. https://doi.org/10.1111/jpy.12027

Steneck, R. S. (1982). A LIMPET-CORALLINE ALGA ASSOCIATION: ADAPTATIONS AND DEFENSES BETWEEN A SELECTIVE HERBIVORE AND ITS PREY'. *Ecology*, *63*(2), 507–522.

Teba Gil-Diaz, Ricardo Haroun, Fernando Tuya, Se´fora Betancor, M. A. V.-R. (2014). Effects of Ocean Acidification on the Brown Alga Padina pavonica : Decalcification Due to Acute and Chronic Events. *PLOS ONE*, *9*(9). https://doi.org/10.1371/journal.pone.0108630

Thivy, F. (1959). ON THE MORPHOLOGY OF THE GAMETOPHYTIC GENERATION. *Marine Biology*, *1*(38), 69–76.

Wang, L., Fan, Y., Parsons, R. L., Hu, G., Zhang, P., & Li, F. (2018). A Rapid Method for the Determination of Fucoxanthin in Diatom A Rapid Method for the Determination of Fucoxanthin in Diatom. *Marine Drugs*, *16*(1), 33. https://doi.org/10.3390/md16010033

Wray, J. L. (1977). *Calcareous Algae*. Amsterdam.

Wright S.W., Jeffrey S.W., Mantoura R.F.C., Llewellyn C.A., Bjørnland, R. D. and, & N., W. (1991). Improved HPLC method for the analysis of chlorophylls and carotenoids from marine phytoplankton. *MARINE ECOLOGY PROGRESS SERIES*, *77*, 183 – 196.

Index

Figures

Figure 8: Boxplot of the relation between R and LC with median (solid line). R changes significantly with LC. n=195 (LC1=47, LC2=69, LC3=34, LC4=45), $p<0,05$ (0,00218 - tested with ANOVA).

Figure 9: Scatter diagram of the relation between R and carbonate with trend line. R changes significantly in relation to the amount of carbonate. n=199, $p<0,05$ (0,00175 - tested with linear regression analysis and spearman test).

Figure 10: Scatter diagram of the relation between R and carbonate per area with trend line. R does not change significantly in relation to the amount of carbonate per area. n=199, $p>0,05$ (tested with regression analyses).

Figure 11: Boxplot of LC in relation R and T to LC with median (solid line). R decreases significantly with LC. n=194 with LC1=47, LC2=68, LC3=34, LC4=45; $p<0,0022$ - tested with ANOVA.
T increases significantly with LC. n=127 with LC1=28, LC2=64, LC3=10, LC4=25; $p<0,0002$ - tested with ANOVA.
R and transmission do not correlate significantly with each other. n=127
$P = 0,7782$ - tested with linear regression analyses.

Figure 12: T spectra of transmitted light (%) in relation to wavelength (nm) in all LC. The T graph mirrors the A graph. It decreases between 400 nm and 500 nm and increases until 650 nm. It has a minimum at 630 nm and raises until 700 nm.

Figure 13: Scatter diagram of the relation between T and A with trend line. A decreases with T. n=127, $p<0,01$ (tested with regression analyses).

Figure 14: A spectra of absorbed light (%) in relation to wavelength (nm) in all LC. The A graph shows an increase between 400 nm am 500 nm and a decent until 650 nm, with a little peak at 630 nm. From 650 nm until 680 the graph raises and falls until 700 nm.

Figure 15: Scatter diagram of the relation between R and A with trend line. A decreases with R. n=127, $p<0,01$ (tested with regression analyses).

Figure 16: bar graph of LC in relation carbonat content, WC and content of organoc substance in relation to each other. Carbonate increases significantly in relation to both with LC. While OM stays at the same level in all LC, the percentage of water in the thallus decreases.
Carbonate to OM: n=199, p<0,01 (tested with regression analyses).
Carbonate to WC: n=199, p<0,01 (tested with regression analyses).

Tables

Table 1: Mean values ± standart division (SD) FM and DM increase significantly with increasing LC.

p_FM = < 0,01

p_DM = < 0,01

n_FM and DM = 199

Table 2: Mean values ± standart division (SD). All compounts in LCs. All componts, except of carbonate per area, increase significantly with LC. Only carbonate per area increases just slightly but not significant.
p_ area, OM, WC, carbonate, carbonate per DW = <0,01
p_ carbonate per area = 0,095
n_ area, OM, WC, carbonate, carbonate per DW, carbonate
per area = 199

Table 3: Mean values ± standart division (SD). R, T and A with LC. R decreases significantly with LC. T increases significantly with LC. A increases slightly with LC (not significant).
p_ R = 0,022, p_ T = 0,002, p_ A =0,077
n_ R = 194, n_ T = 127, n_ A = 127
Significances were measured by ANOVA.

Attachment

Index

Figure 1: Light in percent at depth between zero and twelve meters.

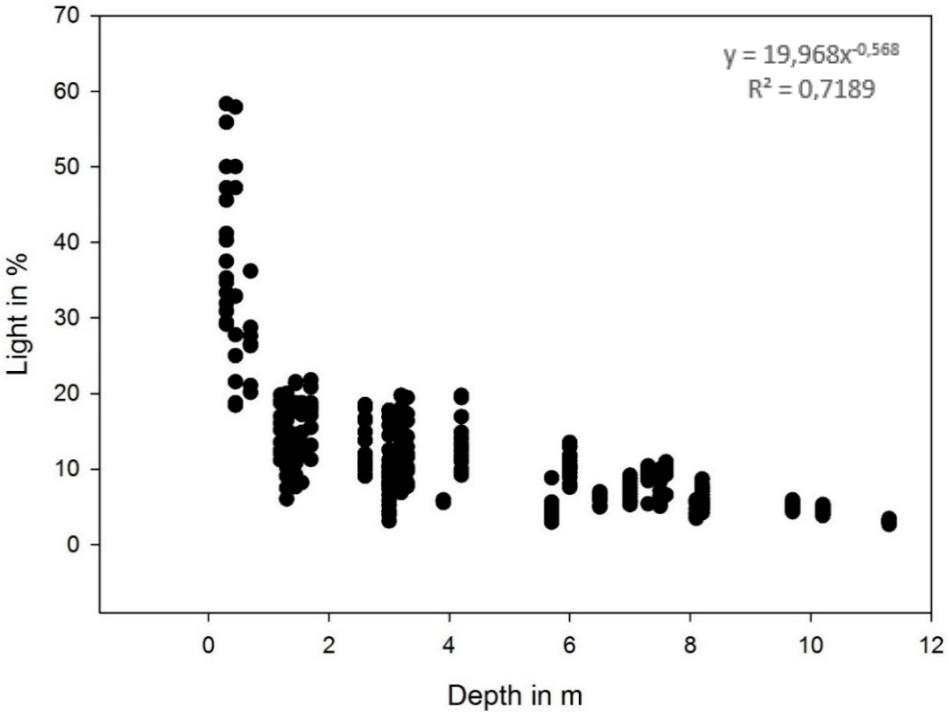

Significance was measured by regression analyses (p<0,01).

Figure 2: The absolute amount of carbonate increases with depth with a slight decline at LC4.

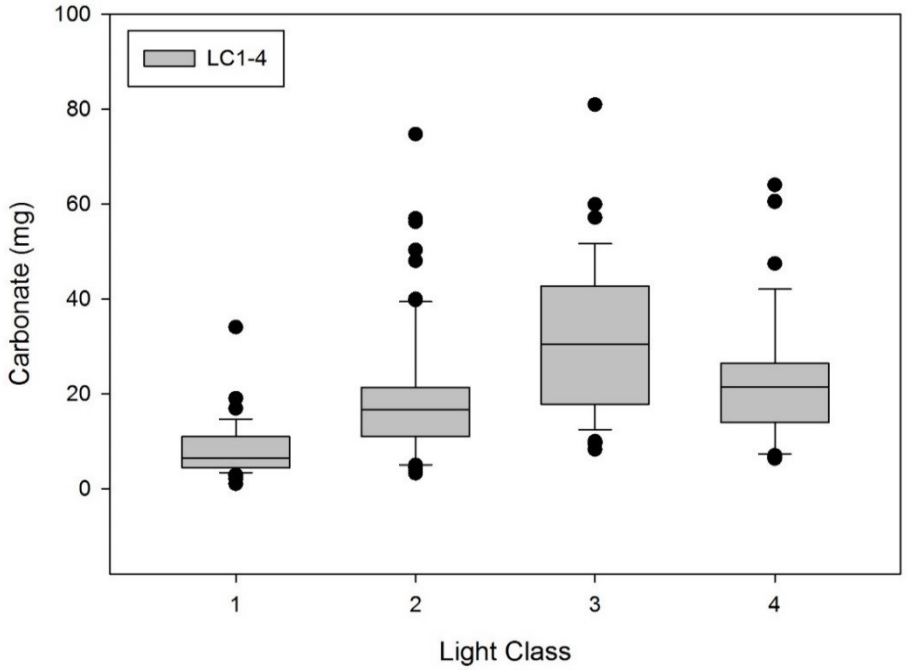

Significance was measured by analyses of variance (ANOVA) (p<0,01)

Figure 3: The absolute amount of carbonate increases with area.

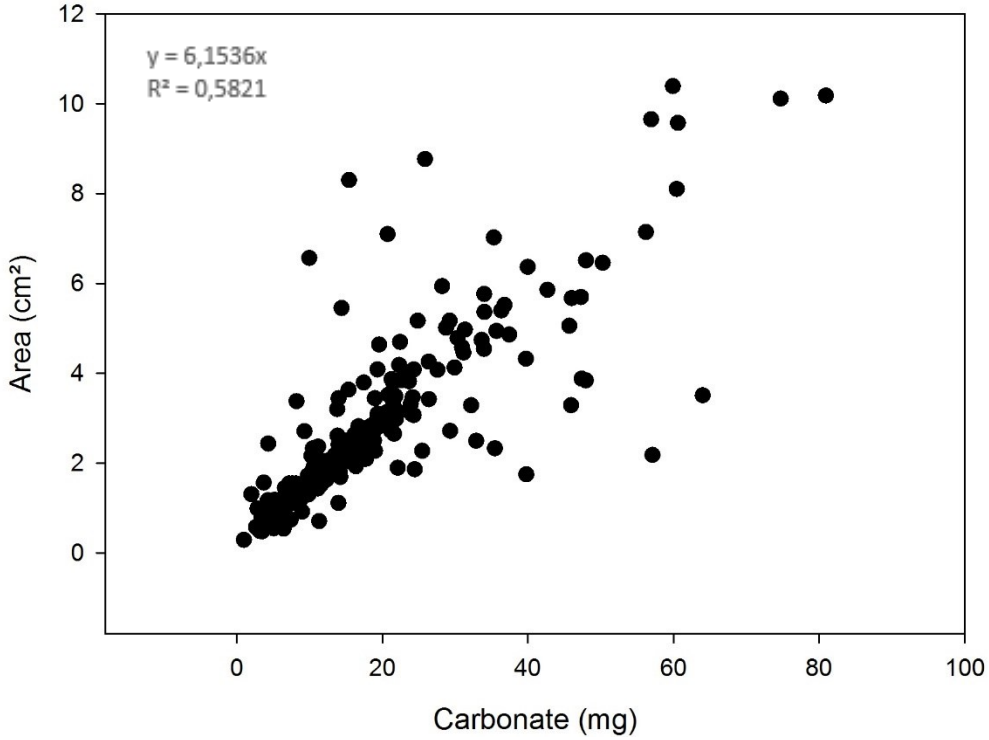

Significance was measured by regression analyses (p<0,01).

Figure 4: The absolute amount of carbonate increases with DM.

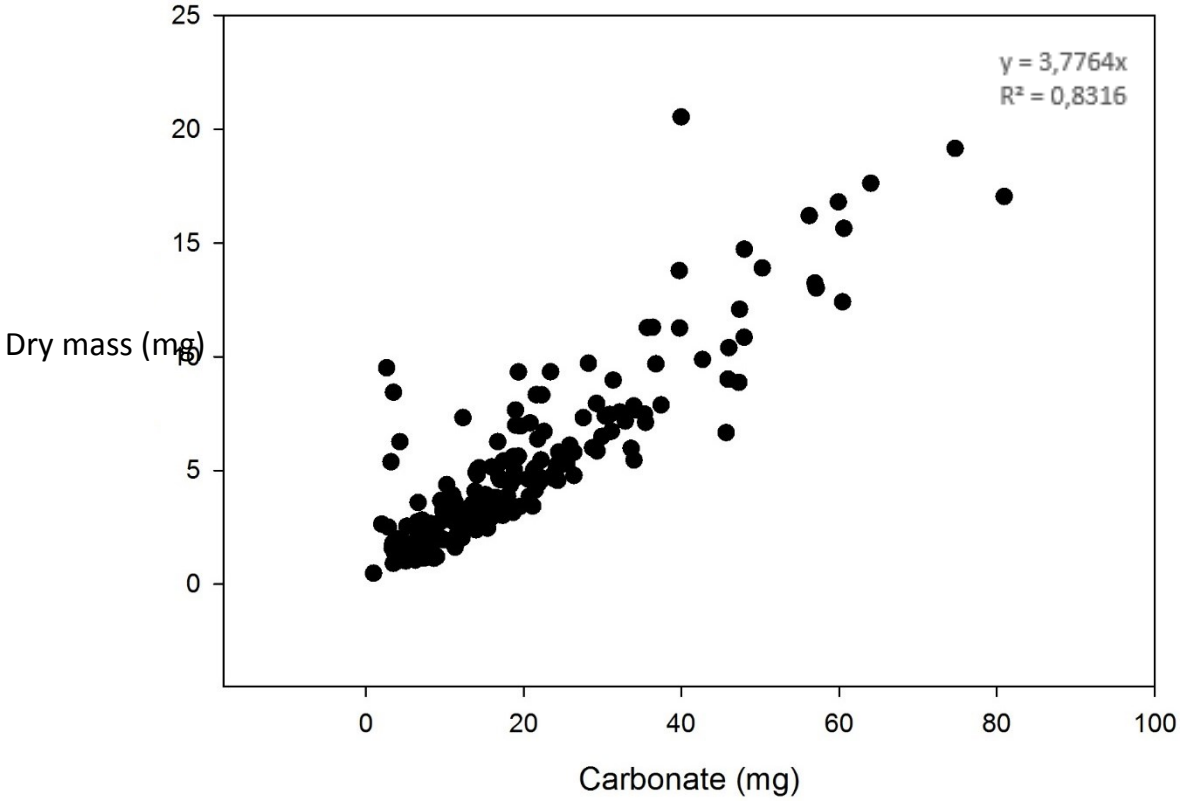

Significance was measured by regression analyses (p<0,01).

Figure 5: The relative amount of carbonate to area does not change significantly with LC.

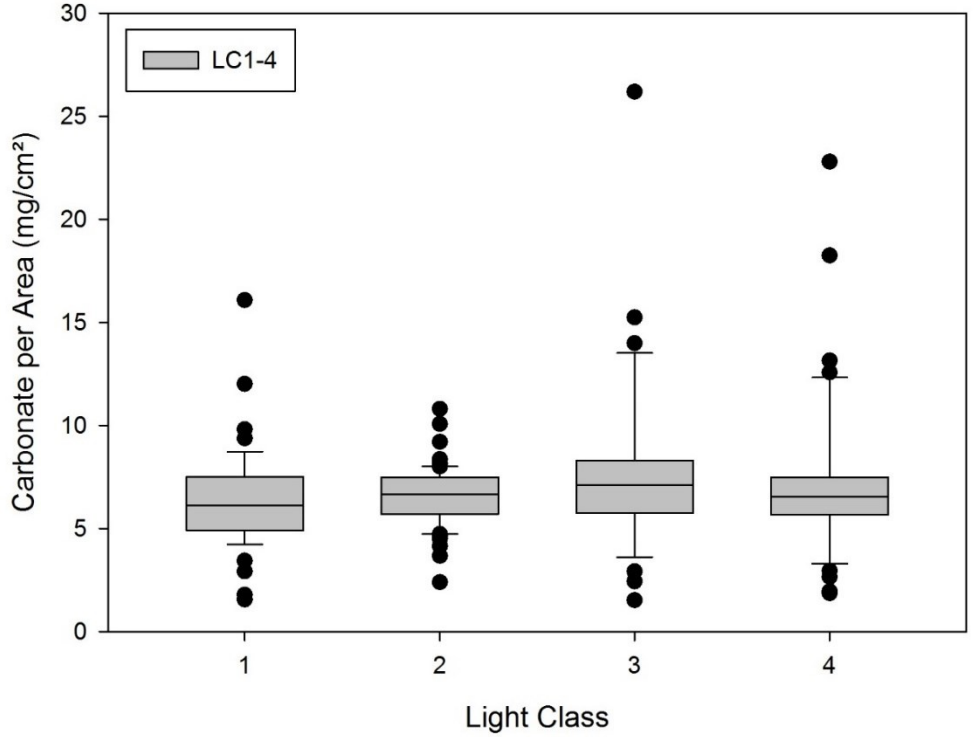

Significance was measured by ANOVA (p>0,05 (0,06913056)).

Figure 6: The relative amount of carbonate to DW changes significantly with LC

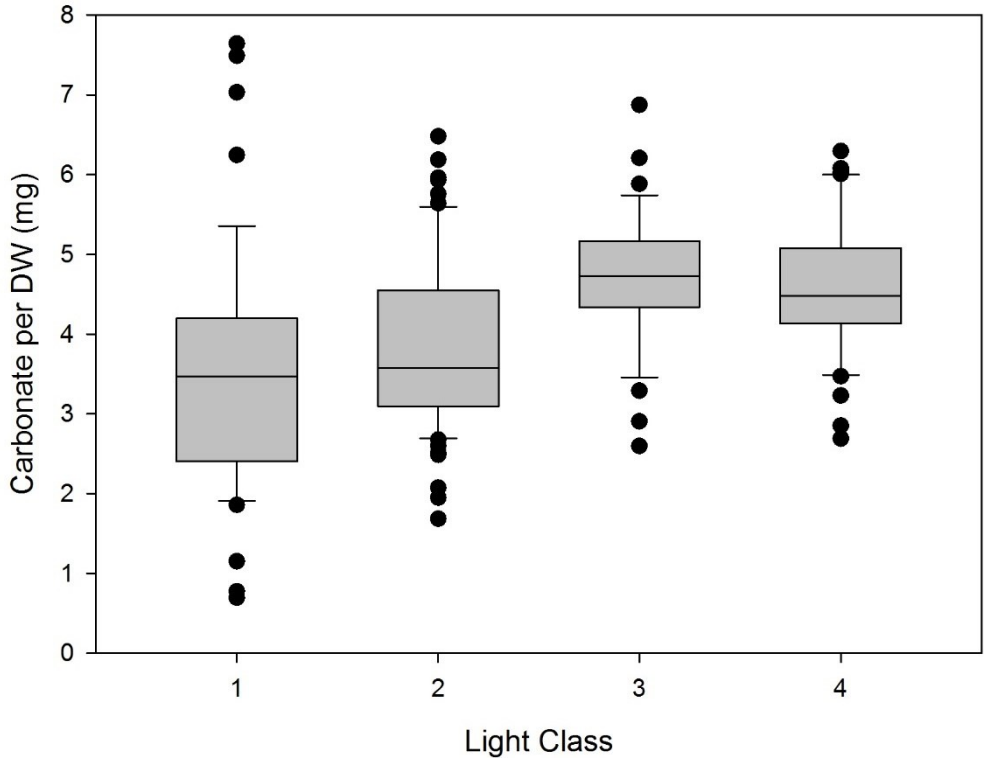

Significance was measured by ANOVA (p<0,01).

Figure 7: The R-Spectrum shows a drop from 400nm to 500nm. From 500nm remain on the same level until 540nm, although a slight increase is visible. From 540nm, all curves drop down with a minimum around 640nm. Finally, the curves increase until 700nm.

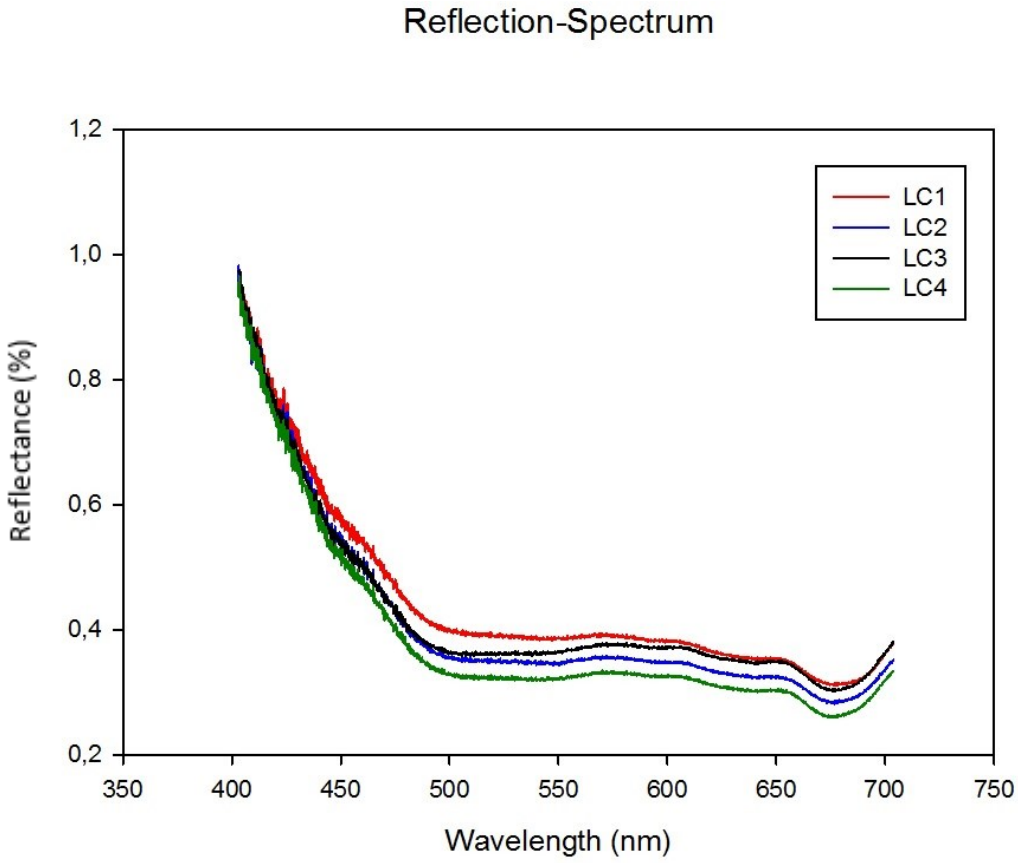

Figure 8: Significant correlation between R and LC

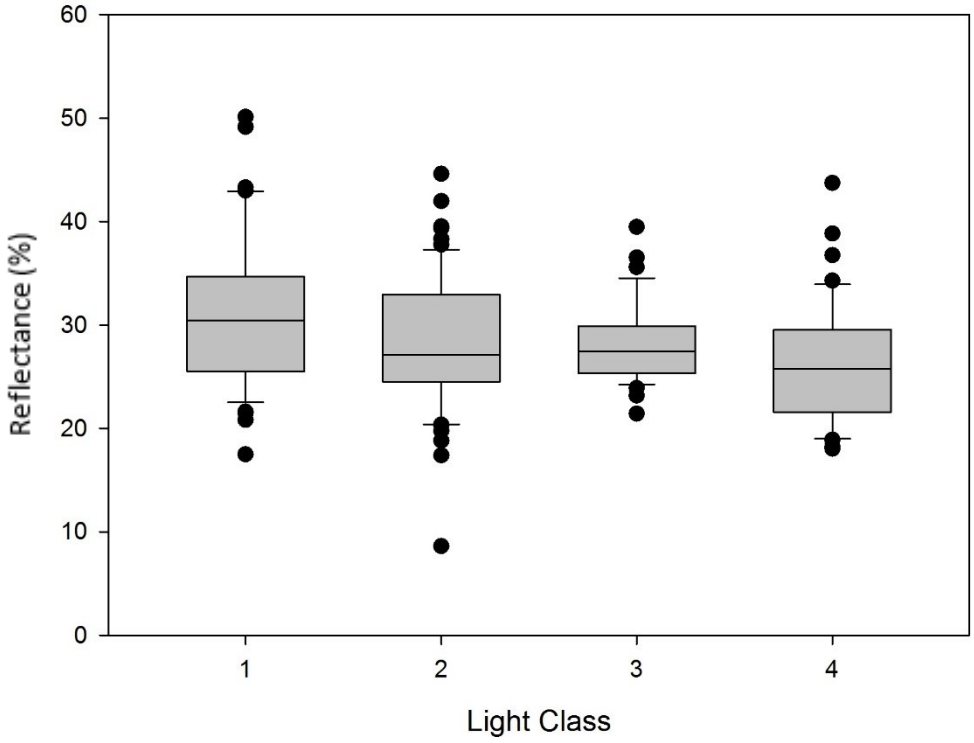

Significance was measured by ANOVA ($p<0,05$ (0,00217916))

Figure 9: The absolute amount of carbonate correlates significantly with refection.

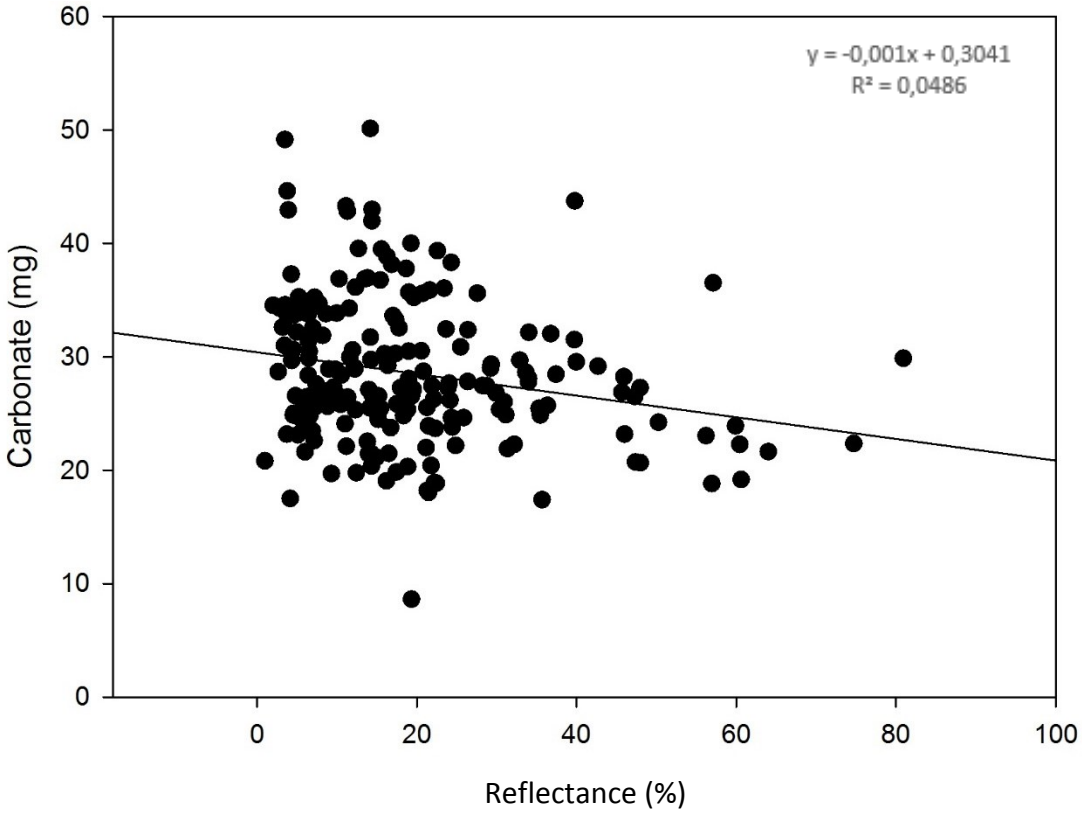

Significance was measured by analyses of linear regression (p<0,05 (0,00174694)).

Figure 10: R does not change in relation to the amount of carbonate per area.

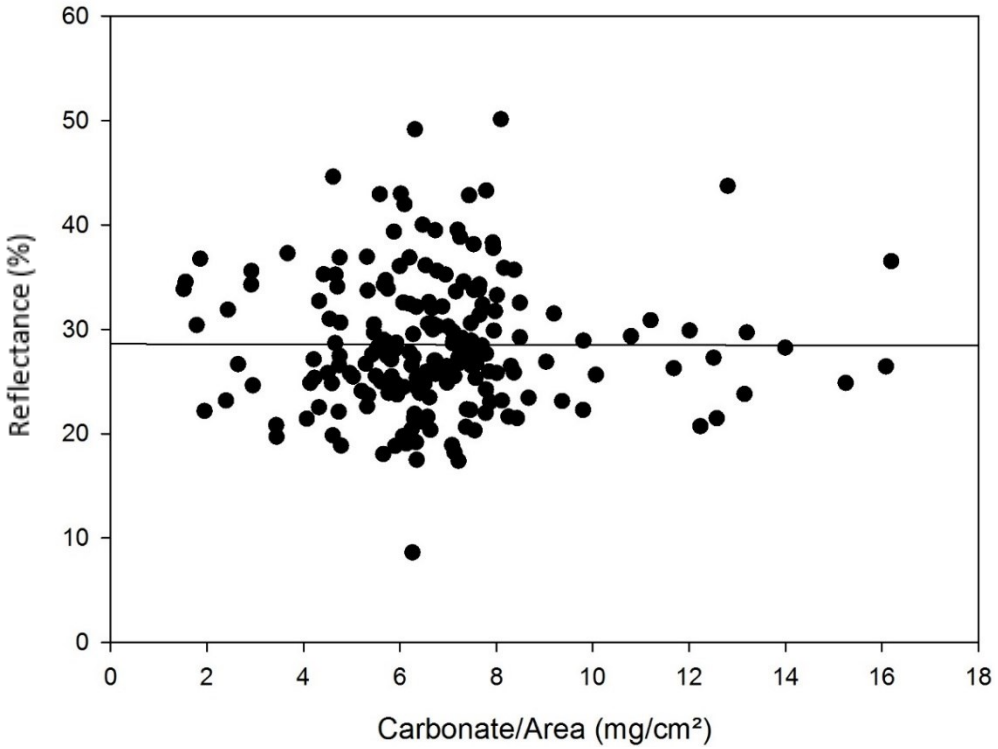

Significance was measured by analysis of regression (p>0,05).

Figure 11: R decreases significantly with LC. T increases, but not significantly with LC. Both have no significant correlation to each other.

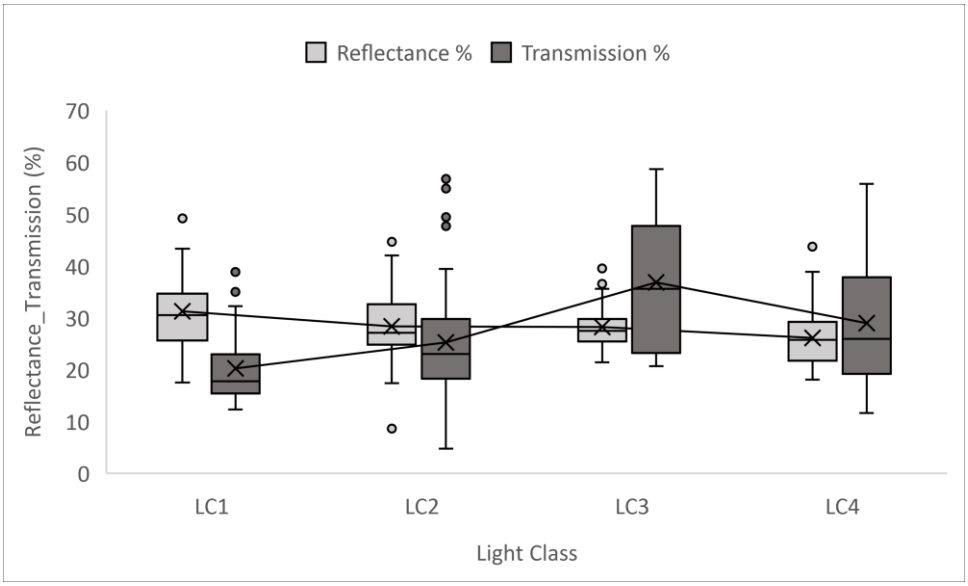

Significances were measures by linear regression analyses.

Figure 12: The T graph mirrors the A graph. It decreases between 400 nm and 500 nm and increases until 650 nm. It has a minimum at 630 nm and raises until 700 nm.

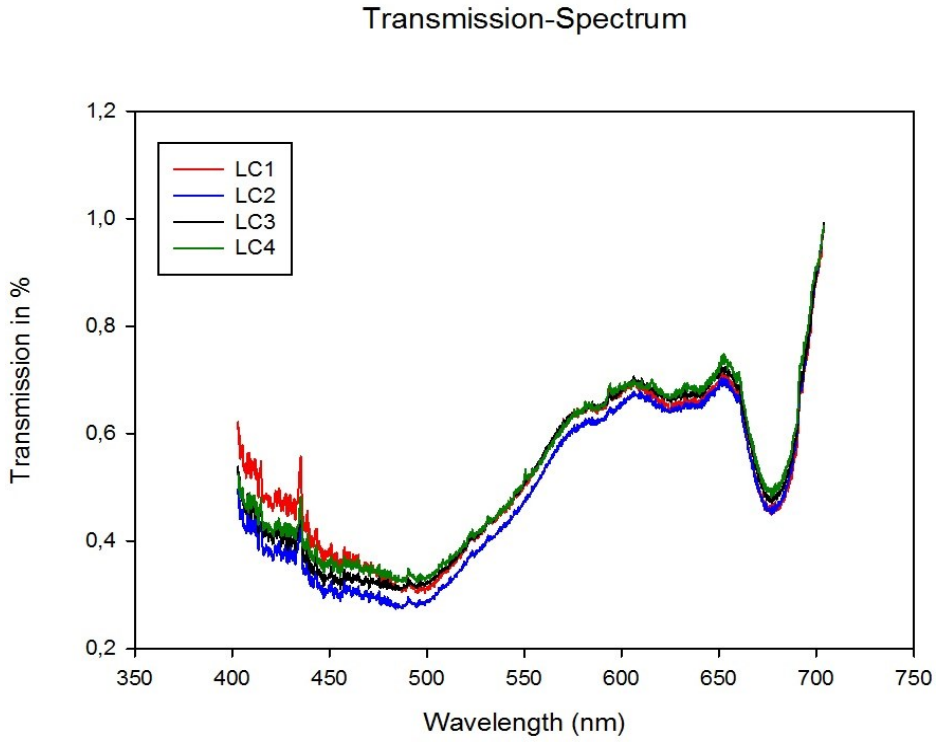

Figure 13: A correlates negative and significant with T.

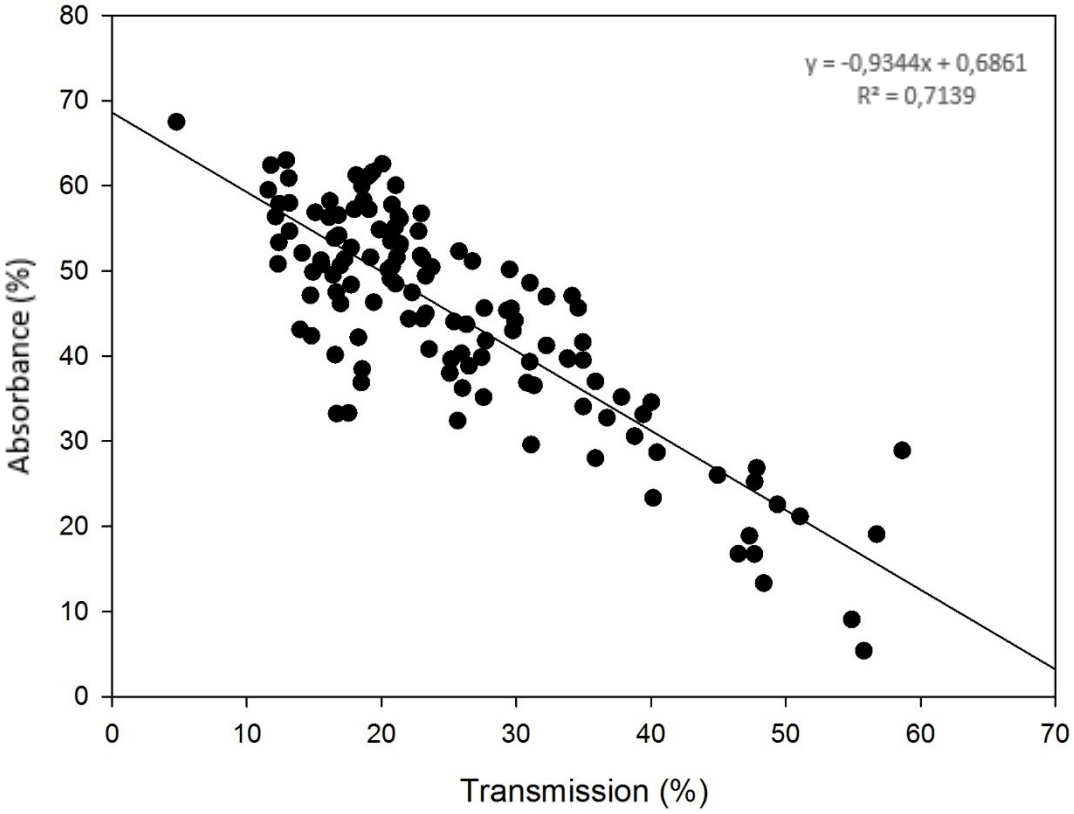

Significance was measured by linear regression analyses ($p<0,01$).

Figure 14: The A graph shows an increase between 400 nm am 500 nm and a decent until 650 nm, with a little peak at 630 nm. From 650 nm until 680 the graph raises and falls until 700 nm.

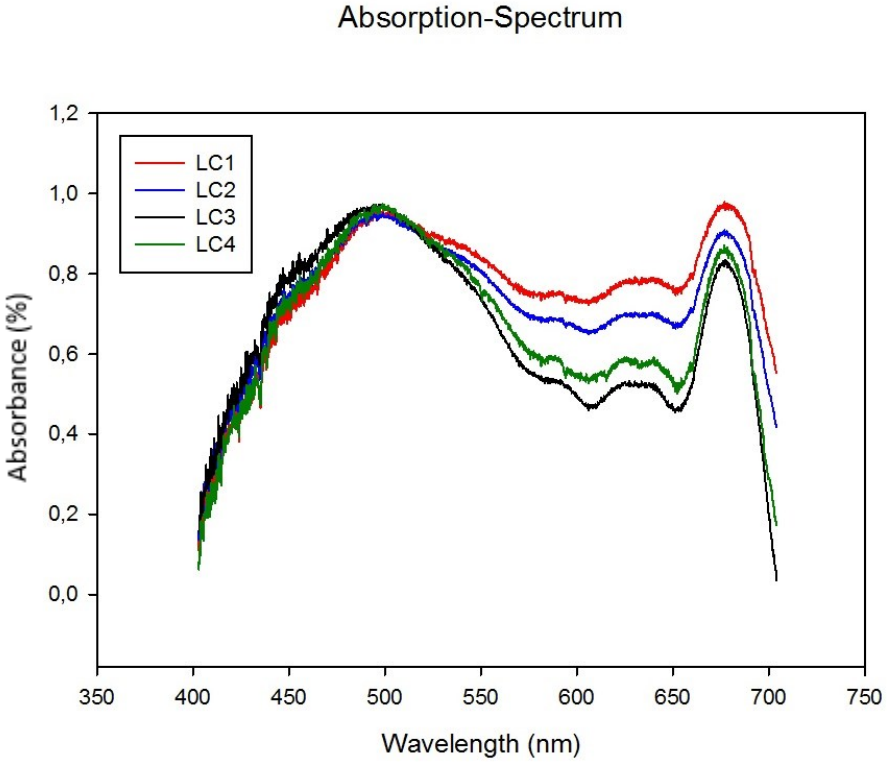

Figure 15: A decreases significantly with R.

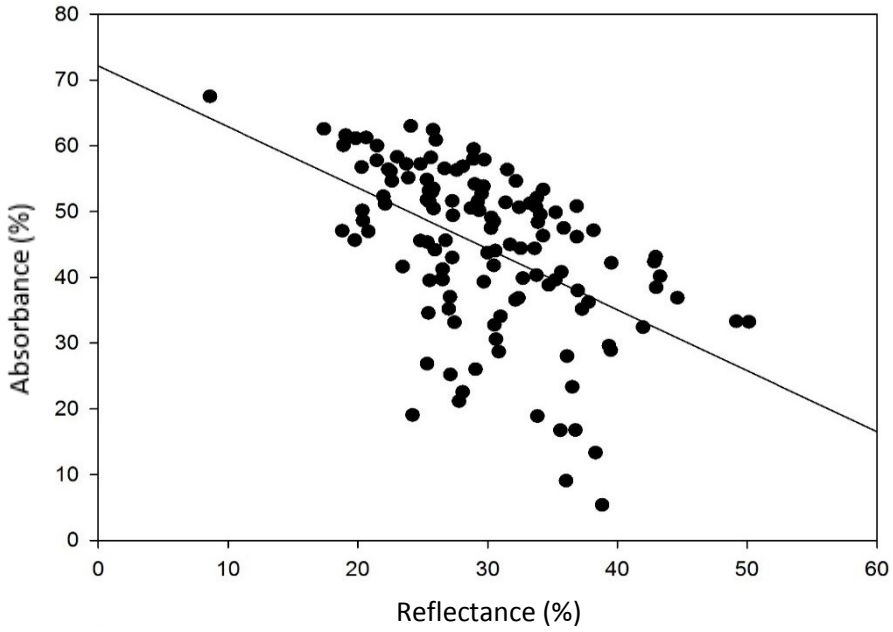

Signicicance was measured by linear regression analyses.

Figure 16: In relation to OM and WC, carbonate increases significantly with increasing LC.

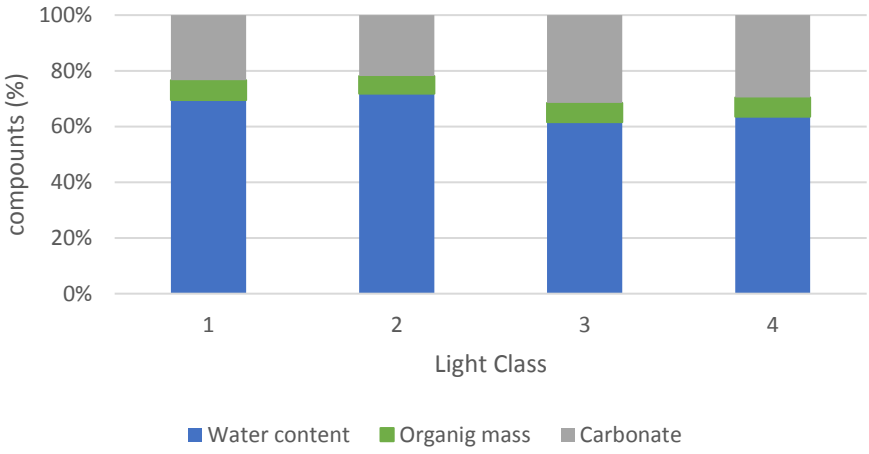

Significances were measured by linear regression analyses (both p-values (carbonate to OM and carbonate to WC) <0,01).

Table 1: FM and DM increase significantly from LC1 to LC3 and decrease from LC3 to LC4.

LC	Fresh Mass	Dry Mass
	mean +/- SD	mean +/- SD
LC1	39,32 +/- 29,29	10,69 +/- 7,16
LC2	89,86 +/- 75,78	24,27 +/- 17,72
LC3	131,77 +/- 71,92	38,51 +/- 19,47
LC4	94,10 +/- 56,51	28,07 +/- 17,28
P:	signif. (< 0,01)	signif. (p< 0,01)

Significances were measured by ANOVA.

Table 2: All compounts in LCs. All componts, except of carbonate per area, increase significantly from LC1 to LC3 and decrease from LC3 to LC4. Only carbonate per area increases just slightly but not significant.

	Area		Organic Substance		Water Content		Carbonate		Carbonate/Area		Carbonate/DW	
	mean	± *SD*	*mean*	± *SD*	*mean*	± *SD*	*mean*	± *SD*	*mean*	± *SD*	*mean*	± *SD*
LC1	1,322	0,901	2,480	1,581	24,343	22,995	8,307	5,855	6,380	2,397	3,508	1,546
LC2	2,814	1,867	5,376	4,343	61,956	60,483	19,108	13,639	6,592	1,405	3,850	1,054
LC3	4,441	2,102	6,916	3,713	61,673	40,500	32,277	15,640	7,858	4,408	4,699	0,865
LC4	3,658	2,487	5,332	3,682	48,940	28,902	21,902	12,608	7,219	3,765	4,581	0,856
P:		signif. (<0,01)		signif. (<0,01)		signif. (<0,01)		signif. (<0,01)	0,095	n. singnif. (>0,05)		signif. (<0,01)

Significances were measured by ANOVA.

Table 3: R decreases with LC. T increases with LC. A increases slightly with LC.

	Reflectance		Transmission		Absorbance	
	mean ±	*SD*	*mean* ±	*SD*	*mean* ±	*SD*
LC1	0,312	0,073	0,202	0,068	6,424	2,404
LC2	0,283	0,065	0,252	0,104	6,609	1,408
LC3	0,281	0,039	0,368	0,140	8,018	4,371
LC4	0,262	0,059	0,289	0,124	7,214	3,808
P:	0,0022	signif. (<0,05)	0,0002	signif. (<0,05)	0,0770	n. singnif. (>0,05)

Significances were measured by ANOVA.

Zusammenfassung

Die kalzifizierende Braunalge *Padina pavonica* ist eine von nur zwei bekannten Braunalgen, die kalzifizieren bzw. eine Thallus–Karbonatauflage bilden.

In dieser Diplomarbeit geht es um die Frage, warum *P. pavonica* kalzifiziert. Die Hypothese lautet, dass die Kalkauflage als Sonnenschutz dient. Individuen, welche in geringerer Wassertiefe wachsen und welche daher höherer Strahlung ausgesetzt sind, sollten daher eine höhere Kalziumkarbonatschicht aufweisen als tiefer wachsende, weniger strahlenexponierte Individuen. Mit einer dickeren Kalkauflauflage sollte weiters, mehr Strahlung reflektiert werden. Es wurde erwartet, dass sich sowohl der Anteil an transmittiertem, als auch an absorbiertem Licht, mit abnehmender Reflexion bzw. mit geringerer Strahlungsexposition erhöhen sollte.

Weiters sollte untersucht werden, ob eine erhöhte Kalkauflage bzw. die dadurch erhöhte Strahlungsreflexion zu vergleichsweise reduzierter Biomasseproduktion führt. Tiefer wachsende, bzw. weniger strahlungsexponierte Exemplare sollten daher größer und schwerer sein. Aufgrund der temperaturabhängigen Wachstumsgeschwindigkeit sollten vergleichsweise große, tiefwachsende Exemplare älter sein als Exemplare naher der Oberfläche.

Die Untersuchungen und das Samplen wurde in Rovinj (Kroatien) im Juni 2018 durchgeführt. Innerhalb von drei Wochen wurden mittels Apnoetauchen Exemplare entnommen und im Labor des Rudjer Boskovic Institute, Kroatien, untersucht. Die erhaltenen Gewichtsmessungen (Frischgewicht, Trockengewicht, Wasseranteil, Kalziumkarbonatgewicht) zeigen eine Zunahme mit Abnahme der

Strahlungsexposition. Auch die Thallusfläche nahm im gleichen Ausmaß zu. Die Menge an Karbonat, welche mittels Lösung durch Essigsäure entnommen wurde, zeigte also nicht die erwartete Abnahme mit reduzierter Strahlung und auch die Reflexionsmessungen, welche mittels Spektroradiometer (*Ocean Optic: USB4000 Miniature Fibre Optic* Spectrometer) durchgeführt wurden zeigten keine signifikanten Korrelationen zu Strahlungsexposition. Die Transmission zeigte hingegen die erwartete Abnahme mit zunehmender Strahlungsreduktion, wohingegen die Absorption konstant blieb. Dies kann auf einen reduzierten Pigmentgehalt und eine Reduktion der Thallusdicke zurückgeführt werden. Zu Beginn der Wachstumsperiode von *Padina* (April bis September), konnte die Sonnenschutzfunktion, der Kalzifikation, daher nicht festgestellt werden. Diese könnte sich jedoch im Laufe der Wachstumsperiode entwickeln. Auf Grund der, trotz konstantem relativem Kalkgehalt (Kalk pro Fläche), größeren und schweren Exemplare in tieferen, weniger lichtexponierten Regionen, kann angenommen werden, dass tieferwachsende Exemplare weniger gezeiten- und wellenexponiert sind und daher ungestörter und, aufgrund der Temperaturreduktion, langsamer wachsen.